JMEPEG (2015) 24:2234–2239
DOI: 10.1007/s11665-015-1491-4

1059-9495/$19.00

Ultrasonic-Assisted Synthesis of Graphite-Reinforced Al Matrix Nanocomposites

P. Christy Roshini, B. Nagasivamuni, Baldev Raj, and K.R. Ravi

(Submitted November 2, 2014; in revised form February 3, 2015; published online April 14, 2015)

A novel approach to produce Al-2 vol.% graphite nanocomposites using micron-sized graphite particles has been reported using conventional stir casting technique combined with ultrasonic treatment. Microstructural observations indicate that the visible agglomerations and porosities are significantly reduced after ultrasonic treatment. Transmission electron microscopy studies of ultrasonic-treated composites reveal that the size of the graphite particles is reduced substantially and its morphology is transformed into flake type structures. The width of the graphite flakes is reduced markedly with the increase in ultrasonic processing time and it is found to be in the range of 100-120 nm with an aspect ratio of 8.83 after 5 min of ultrasonication. Added to that, considerable improvement in the hardness values are noted for ultrasonic-treated Al-2 vol.% graphite composites when compared to conventional untreated composites. The mechanism behind the significant reduction in graphite particle size and porosity, uniform distribution of graphite particles and hardness increments are discussed.

Keywords aluminum, advanced characterization, composites, metallic matrix, nanomaterials, nanoprocessing

1. Introduction

Metal matrix composites (MMCs) combine the properties of ceramics (high strength, high modulus, and wear resistance) with those of metals or alloys (ductility and toughness) to produce significant improvements in the mechanical properties of the composite over those of the monolithic metal or alloys (Ref 1). Currently, several ceramic reinforcement particles such as SiC, B_4C, AlN, Al_2O_3, SiO_2, TiC, TiB_2, and graphite are used to fabricate MMCs (Ref 1, 2). Among these, graphite has been recognized as a high strength and low density material, thus providing engineers with cost-effective Al-Graphite composites used in automotive components like bushes and bearings (Ref 3). However, most of the available Al-Graphite MMCs have reinforcement particles with size ranging from tens to hundreds of microns (Ref 4, 5) which result in substantial reduction in ductility and toughness (Ref 6). The poor ductility of MMCs limits their application in areas where good ductility and formability are required (Ref 5, 6). Recent studies emphasize that incorporation of nanosized particles in the metal matrix significantly improves the strength without an appreciable decrease in ductility and toughness, which leads to the fabrication of metal matrix nanocomposites (MMNCs) (Ref 7).

Currently, several methods are available for the production of MMNCs including mechanical alloying (Ref 2), severe plastic deformation (Ref 8), spray deposition (Ref 9, 10), and solidification processing (Ref 11). Among these methods, solidification-processing (e.g., casting) is the cost-effective approach for large-scale processing of metals; hence, there is a significant interest toward casting-based approach to fabricate MMNCs (Ref 11). However, the fabrication of MMNCs based on solidification-processing method causes the nanoparticle agglomeration due to high surface energy and results in non-uniform distribution of particles in the metal matrix (Ref 12). Recently, ultrasonic treatment (Ref 11, 13-15) has been reported to overcome the above cited problems through non-linear effects giving rise to cavitation and acoustic streaming mechanisms.

Li et al. (Ref 16-24) extensively investigated the effects of ultrasonic treatment in the fabrication of both Al and Mg matrix ex situ nanocomposites and reported that the strength of the materials can be improved without much loss in ductility. Effective dispersion and breakage of agglomerates of SiC nanoparticles in A356 matrix has been reported due to ultrasonic treatment (Ref 11, 16, 17). Similar studies in Mg/SiC nanocomposites showed a better yield and tensile properties with the assistance of ultrasonic treatment (Ref 18-22). Other than SiC, Al_2O_3 (Ref 23) and TiB_2-reinforced nanocomposites (Ref 24) were also reported to have improved mechanical properties. In addition to that, the porosity levels are also suggested to decrease because of the degassing effect of ultrasonic treatment (Ref 16, 17).

The effects of ultrasound are prominently explored in chemical engineering and applied chemistry not only for dispersing the nanoparticles (Ref 25) but also to generate nanoparticles from micron-sized particles (Ref 26). Especially, it is reported that ultrasonication aids in exfoliation of graphite to form thin flakes of graphite nanosheets (Ref 27). Similarly, graphite has been exfoliated with different agents like Sodium dodecyl benzene sulfonate (Ref 28, 29), formic acid (Ref 30), and silicate (Ref 31) with the aid of ultrasonic treatment. It is reported that graphite

This article is an invited paper selected from presentations at "Innovation in Processing of Light Metals for Transportation Industries: A Symposium in Honor of C. Ravi Ravindran," held during MS&T'14, October 12-16, 2014, in Pittsburgh, PA, and has been expanded from the original presentation.

P. Christy Roshini, B. Nagasivamuni, and **K.R. Ravi**, Structural Nanomaterials Laboratory, PSG Institute of Advanced Studies, Coimbatore - 641 004, Tamil Nadu, India; and **Baldev Raj**, Structural Nanomaterials Laboratory, PSG Institute of Advanced Studies, Coimbatore - 641 004, Tamil Nadu, India and National Institute of Advanced Studies, Bangalore - 560 012, Karnataka, India. Contact e-mail: krravi.psgias@gmail.com..

particles can be tailored into different forms under ultrasonic treatment confined to medium characteristics (Ref 27-31).Therefore, the present work is focused to investigate the influence of ultrasonic melt treatment during synthesis of Al-2 vol.% graphite composites. The role of ultrasonic treatment time on dispersion of graphite particles and porosity has been examined. Mechanism of ultrasonic treatment on microstructural evolution of graphite nanoparticles in Al-Gr_p composites has been discussed.

2. Experimental Procedure

Pure aluminum (99.7% commercial purity) and graphite powders with average particle size of 20.89 ± 3.89 μm (Fig. 1) were used to synthesize Al-2 vol.% graphite microcomposite by conventional stir casting technique. After adequate stirring of the melt, the preheated ultrasonic probe was dipped into the melt and sonicated for 1, 3, and 5 min. A high power ultrasonic probe (Hangzhou Success, China), made of Ti-6Al-4V, was used to generate a 20 kHz and 2.5 kW power input for ultrasonic treatment process. The composite melt was then poured into cast iron mold. For comparison, the composite sample without ultrasonic treatment was also cast.

The samples for microstructure analysis were sectioned at 20 mm from the bottom of the casting and electro-polished using 2% HBF_4 solution. The polished samples were characterized using polarized light optical microscope (Carl Zeiss Axio Scope A1). The size and morphology of reinforcement particles after ultrasonic treatment were analyzed using JEOL JEM 2100 transmission electron microscopy (TEM) operating at 200 kV. For the TEM analysis, the samples were prepared by Ar-ion milling preceded by dimpling. Hardness of the untreated and ultrasonic-treated Al-2 vol.% graphite composite was measured with Kuang Microhardness tester using a load of 200 g and a dwell time of 10 s. Twenty readings were taken for each sample, and the average value has been reported.

3. Results and Discussion

Optical microscope images of the untreated sample and ultrasonic-treated Al-2 vol.% graphite samples are shown in Fig. 2. Microstructure of untreated stir cast composite shows a significant amount of porosity along with the agglomeration of graphite particles (Fig. 2a). During the processing of Al MMCs using stir cast technique, the molten aluminum is mechanically stirred to create a vortex, which draws the reinforcement together with the ambient gases into the liquid medium. Suction of gases/air along with the particles has been observed by Ramani et al. (Ref 32) while performing experiments with transparent media. When solid reinforcement particles are introduced into the melt along with gas phase, the reinforcement prefers to be attached to the gas phase rather than molten metal, since the interface energy for reinforcement/gas interface is lower than the reinforcement/metal interface. This concept has been widely accepted in the area of metallic foam wherein stabilization of gas phase in the molten metal found to be largely improved in the presence reinforcement particles (Ref 33). The aforementioned discussion clearly explains the microstructural observation of agglomerated graphite particle in the vicinity of porosity (Fig. 2a). However, after 1-minute ultrasonic treatment, the porosities are significantly reduced and the particle clusters have been broken considerably (Fig. 2b). Further increase in ultrasonic treatment time has very less effect on microstructure (Fig. 2c and d). In order to ensure the microstructural observation of a porosity reduction in ultrasonic-treated composites, density measurements are made using Archimede's principle. Figure 3 shows the density of untreated and ultrasonic-treated Al-2 vol.% graphite composites. It is clear that the density of Al-2 vol.% graphite composite is significantly increased within 1 min of ultrasonic treatment. A marginal change in density is observed upon 3 and 5 min of ultrasonic treatment. The maximum density measured after ultrasonic treatment is around 2.68 g/cm^3 which is near to the theoretical density of Al-2 vol.% graphite composite, 2.69 g/cm^3. These results substantiate the microstructurally observed reduction in porosity of ultrasonic-treated Al-2 vol.% graphite composites.

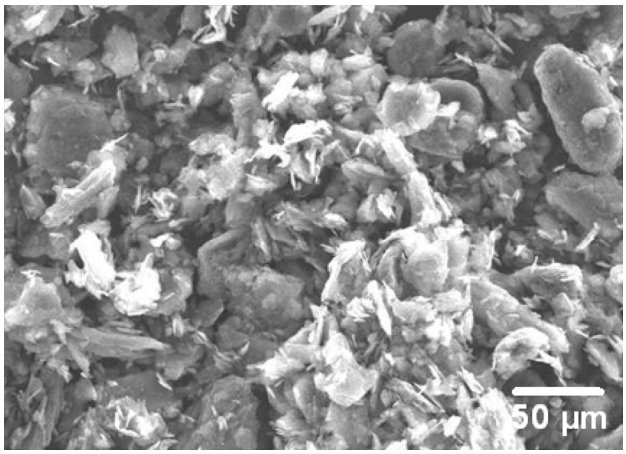

Fig. 1 Scanning electron microscope (SEM) images of as-received graphite particles

In general, when ultrasound is passed through the liquid melt, it imparts significant energy to the molecules in the melt (Ref 11, 16-22). The ultrasound comprises of compression phase, which exerts a positive pressure for pulling the molecule together and rarefaction phase, which exerts negative pressure for pushing the molecules away from each other. During rarefaction phase, small vapor filled voids called cavitation bubbles are formed when the pressure amplitude exceeds the tensile strength of the liquid melt (Ref 34). The formed cavity grows in a few cycles of sound waves and reaches an unstable state that causes the bubble to collapse. The formation, growth, and implosive collapse of bubbles in liquids treated with high frequency sound are called acoustic cavitation. These cavitation effects are found in diverse applications in material and chemical synthesis (Ref 16-22, 34). For such a cavitation-aided implosion to occur in light metals, minimum ultrasonic intensity should lie within 80-100 W cm^{-2} (Ref 11, 16-24). Assuming that the emitter surface is completely wetted by the melt with negligible attenuation, the intensity is given by

$$I = \frac{1}{2}\rho_L c_L (2\pi f A_0)^2 \quad \text{(Eq 1)}$$

where f is the frequency, $\rho_L = 2.333$ g/cm^3 is the density of liquid aluminum, $c_L = 1330$ m/s is the velocity of sound waves through liquid aluminum, and A is the cross section area of sonotrode. Under the operating conditions of 20 kHz

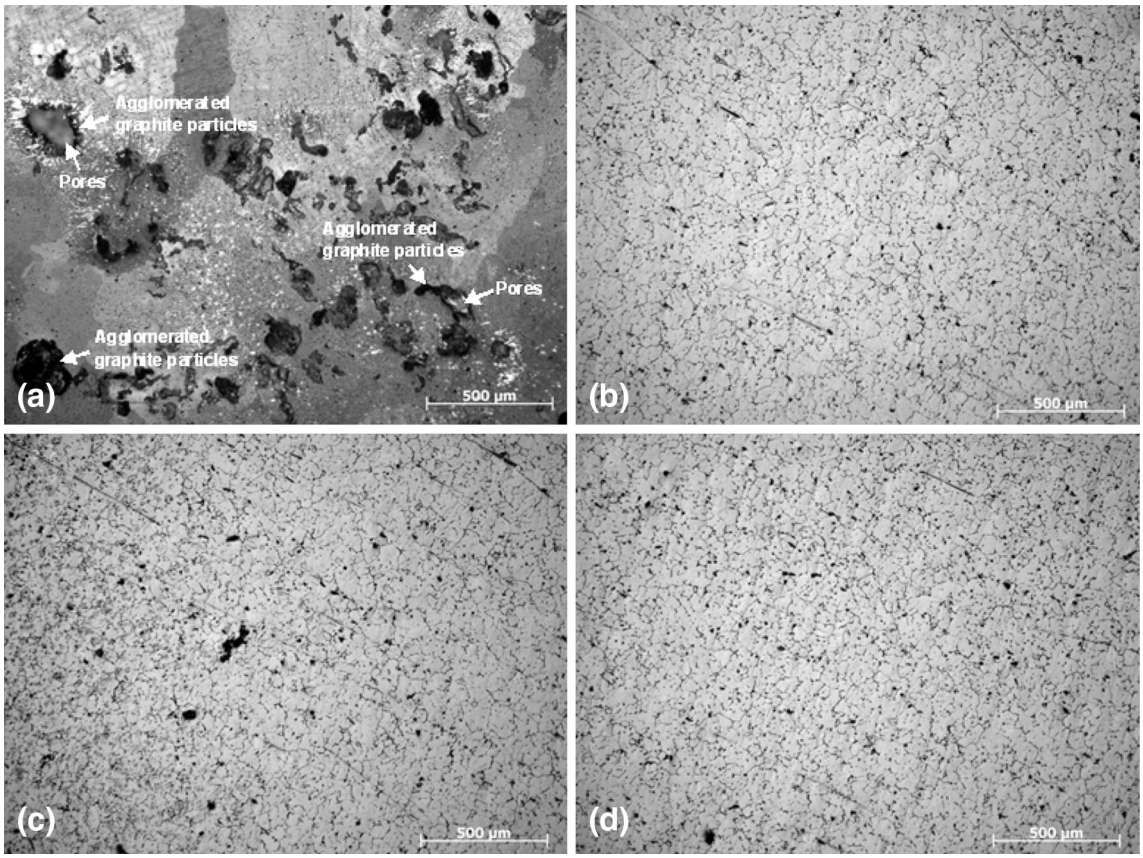

Fig. 2 Optical microscope images of Al-2vol.% graphite nanocomposite in (a) untreated and ultrasonic treated for (b) 1 (c) 3 and (d) 5 min

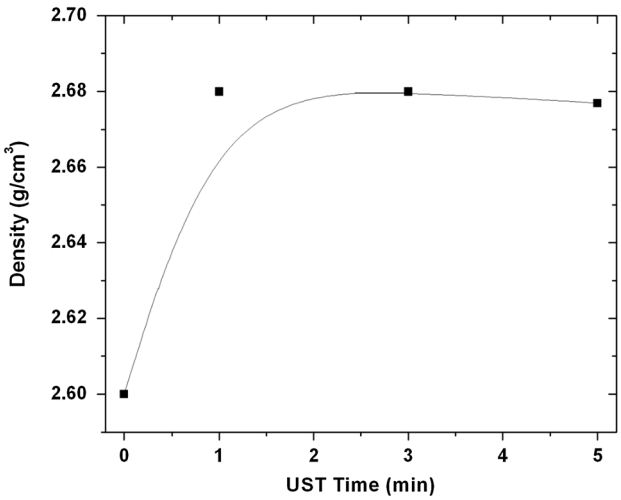

Fig. 3 Density of Al-2vol.% graphite nanocomposites as a function of ultrasonic treatment time

frequency and 6 μm amplitude, the intensity of the radiating surface is calculated as 89.13 W cm^{-2}. It suggests that the occurrences of cavitation related effects are reasonable.

During stir casting of the composites, more number of cavitation sites is introduced into the melt. Particles that are improperly wetted or associated with gas pockets can readily act as cavitation sites during ultrasonic treatment (Ref 35). The explosion of cavitation bubbles attached to the particle surfaces can cause the breakage of particles agglomeration, and series occurrence of such cavitation events can significantly promote the dispersion of the particles (Ref 34). It is also reported that under the influence of fully developed cavitation, degassing effects are accelerated dramatically (Ref 35, 36). In Al melts, the main source of porosity is due to the dissolved hydrogen (Ref 36) and during the processing of the composite using stir casting technique the melt has been subjected to more absorption of these gases. During the compression and rarefaction cycle, part of the bubbles grow in size and floats to the surface (Ref 35, 36). The efficiency of degassing increases from 30 to 60% under cavitation conditions compared to non-developed cavitation ultrasonic treatment (Ref 37, 38). These are the possible reasons for the reduction in porosities and agglomerations observed after ultrasonic treatment of Al-2 vol.% graphite composite.

In order to study the influence of ultrasonic treatment on the size and morphology of graphite, TEM analysis has been carried out on Al-2 vol.% graphite composite. After 1 min of ultrasonic treatment the width of the graphite particles ranges from 250 to 350 nm with an aspect ratio of 7.46 which is a significant reduction from the initial size of as received graphite particles, 20.89 ± 3.89 μm. A gradual reduction is observed in the width of graphite particles from 120-180 to 100-130 nm is observed upon 3 and 5 min of UST as shown in Fig. 4(c) and (d), respectively.

The TEM observations indicate that the size of graphite particles is modified extensively under the influence of physical and mechanical effects imposed by the ultrasonic treatment. Compared to the as-received graphite particles, the ultrasonic-treated composite shows an elongated flake-type morphology.

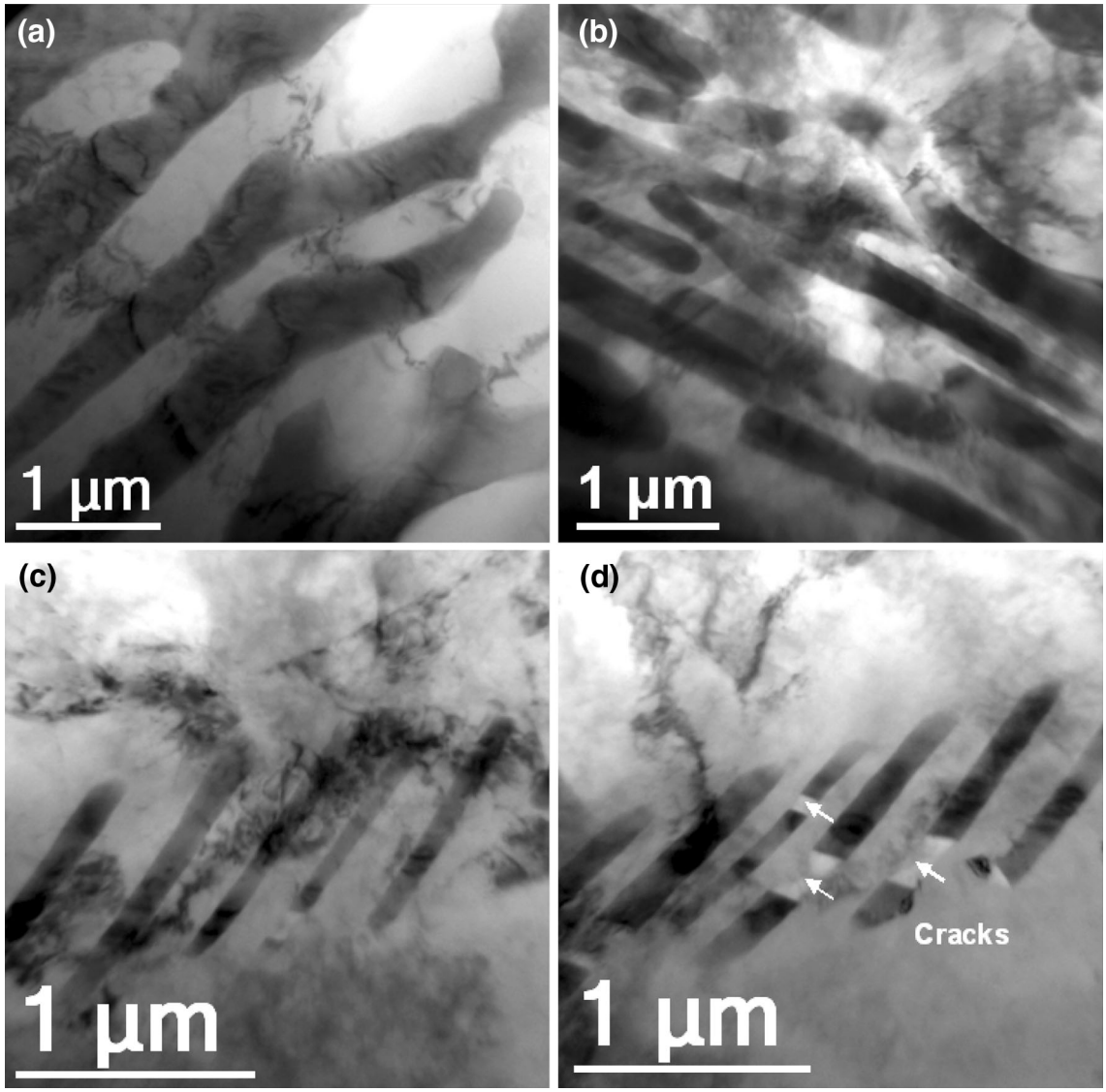

Fig. 4 TEM bright field images of Al-2vol.% graphite nanocomposites ultrasonic treated for (a) 1 (b) 3 and (c) & (d) 5 min

Traditional methods of producing or formation of such graphite flakes are reported in organic solvents or ionic liquids via sonication by either chemical or mechanical method (Ref 39, 40). These methods rely on the physical effects of ultrasound to break the 3D structures of graphite to graphene (Ref 39). It is well known that the carbon atoms in graphite are covalently bonded to each other in hexagonal planar structure with sp^2 hybridization and each planar layer is stacked together along [0001] direction with Vander Waal bond. The Young's modulus of the crystal parallel to the basal plane is 100 times greater than that of the hexagonal axis of [0001] direction. Hence, under fully developed acoustic cavitation, conditions are sufficient to break the Vander Waal interactions between each graphite layer to form an elongated flake-type of structures shown in the Fig. 4(a) and (b). Since the coefficient of thermal expansion of the graphite parallel to the hexagonal axis is 25×10^{-6} K^{-1} and parallel to the basal plane is 1.5×10^{-6} K^{-1}, therefore graphite particles may expand in the melt along [0001] direction (Ref 41). This thermal expansion behavior of graphite particle also can aid the above-mentioned Vander Walls bond breaking process. As the sonication time increases, the width of the flakes reduces significantly. The deformation of graphite particle may also be caused due to the mechanical shockwaves and shear forces created by the violent collapse of bubbles during ultrasonic treatment (Ref 39, 40). As the ultrasonication time is increased, the particle tends to break the basal plane and cracks similar to Mrozowski cracks (Ref 41) may be assumed to have formed in the basal plane (indicated by arrows in Fig. 4d) which breaks the graphite sheets further to form graphite nanoparticles.

Figure 5 shows the microhardness analysis of Al-2 vol.% graphite composite as a function of ultrasonic treatment time. The hardness of as cast composite material increases significantly after 1 min of ultrasonic treatment from 270 ± 19 to 352 ± 11 MPa. Increasing ultrasonic treatment time to 3 and 5 min has shown only marginal increment in the hardness measurements. The significant improvement in hardness observed in the present work is possibly explained in terms of synergistic effects of particle dispersion, size reduction, and degassing caused by ultrasonic treatment. However, elaborate

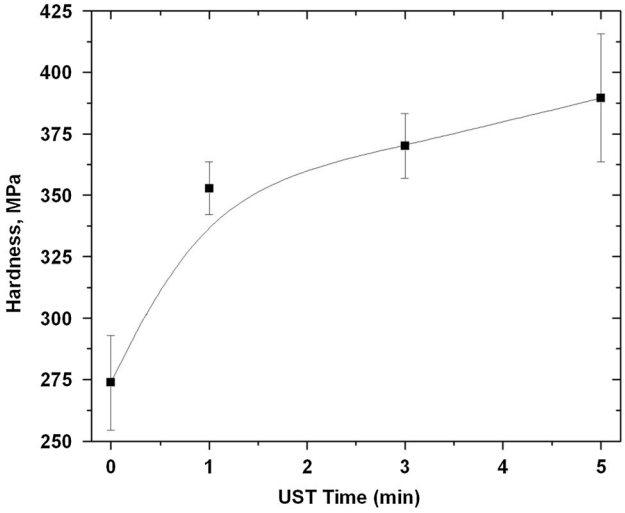

Fig. 5 Hardness of Al-2vol.% graphite nanocomposites as a function of ultrasonic treatment time

studies are still needed to understand the precise strengthening mechanism associated with the ultrasonic treated Al-Graphite nanocomposites.

4. Conclusion

The fabrication of Al-2 vol.% graphite nanocomposites has been demonstrated using conventional stir casting method with the aid of ultrasonic treatment. The agglomeration and porosity problems associated with the conventional stir cast method has been reduced significantly using ultrasonic treatment. Apart from particle dispersion, ultrasonic cavitation also provides the conversion of micron-sized graphite particles to nanosize particles. Notable increase in the hardness of the material is observed after ultrasonic treatment, which may be attributed to the synergistic effects of particle dispersion, size reduction, and degassing.

Acknowledgments

The authors would like to acknowledge the funding support of University Grant Commission (UGC), Government of India under the UGC-DAE CSRscheme (File No: CSR-KN/CRS-34/2012-13/744).

References

1. I.A. Ibrahim, F.A. Mohamed, and E.J. Lavernia, Particulate Reinforced Metal Matrix Composites—A Review, *J. Mater. Sci.*, 1991, **26**, p 1137–1156
2. R. Deaquino-Lara, I. Estrada-Guel, G. Hinojosa-Ruiz, R. Flores-Campos, J.M. Herrera-Ramirez, and R. Martinez-Sanchez, Synthesis of Aluminum Alloy 7075-Graphite Composites by Milling Processes and Hot Extrusion, *J. Alloys Compd.*, 2011, **509S**, p S284–S289
3. N. Barekar, S. Tzamtzis, B.K. Dhindaw, J. Patel, N. Hari Babu, and Z. Fan, Processing of Aluminum-Graphite Particulate Metal Matrix Composites by Advanced Shear Technology, *J. Mater. Eng. Perform.*, 2009, **18**, p 1230–1240
4. U.T.S. Pillai, B.C. Pai, K.G. Satyanarayana, and A.D. Damodaran, Fracture Behaviour of Pressure Die-Cast Aluminium-Graphite Composites, *J. Mater. Sci.*, 1995, **30**, p 1455–1461
5. J. Leng, G. Wu, Q. Zhou, Z. Dou, and X. Huang, Mechanical Properties of SiC/Gr/Al Composites Fabricated by Squeeze Casting Technology, *Scr. Mater.*, 2008, **59**, p 619–622
6. X. Li, Y. Yang, and D. Weiss, *Ultrasonic Cavitation Based Dispersion of Nanoparticles in Aluminium Melts for Solidification Processing of Bulk Aluminum Matrix Nanocomposite: Theoretical Study, Fabrication and Characterization*, American Foundry Society (AFS) Transactions, Schaumburg, 2007, p 1–12
7. R.S. Rana, R. Purohit, and S. Das, Review of Recent Studies in Al Matrix Composites, *IJSER*, 2012, **3**(6), p 1–16
8. M.J. Demkowicz and L. Thilly, Structure Shear Resistance and Interaction with Point Defects of Interfaces in Cu-Nb Nanocomposites Synthesized by Severe Plastic Deformation, *Acta Mater.*, 2011, **59**(20), p 7744–7756
9. D. Huda, M.A.E.I. Bradie, and M.S.J. Hashmi, Metal Matrix Composites: Manufacturing Aspects, Part I, *J. Mater. Process. Technol.*, 1993, **37**, p 513–528
10. J.B. Yang, C.B. Lin, T.C. Wang, and H.Y. Chu, The Tribological Characteristics of A356.2 Al alloy/$Gr_{(p)}$ Composites, *Wear*, 2004, **257**, p 941–952
11. Y. Yang, J. Lan, and X. Li, Study on Bulk Aluminum Matrix Nanocomposite Fabricated by Ultrasonic Dispersion of Nano-sized SiC Particles in Molten Aluminum Alloy, *Mater. Sci. Eng. A*, 2004, **380**, p 378–383
12. S.J. Hong, H.M. Kim, C. Suryanarayana, and B.S. Chun, Effect of Clustering on the Mechanical Properties of SiC Particulate-Reinforced Aluminum Alloy 2024 Metal Matrix Composites, *Mater. Sci. Eng. A*, 2003, **347**, p 198–204
13. Zhiwei Liu, Qingyou Han, and Jianguo Li, Ultrasound Assisted In Situ Technique for the Synthesis of Particulate Reinforced Aluminum Matrix Composites, *Compos. B*, 2011, **42**, p 2080–2084
14. Su Hai, Wenli Gao, Zhaohui Feng, and Lu Zheng, Processing, Microstructure and Tensile Properties of Nano-sized Al_2O_3 Particle Reinforced Aluminum Matrix Composites, *Mater. Des.*, 2012, **36**, p 590–596
15. I. Narasimha Murthy, D. Venkata Rao, and J. Babu Rao, Microstructure and Mechanical Properties of Aluminum-Fly ash Nanocomposites Made by Ultrasonic Method, *Mater. Des.*, 2012, **35**, p 55–65
16. X. Li, Y. Yang, and D. Weiss, Theoretical and Experimental Study on Ultrasonic Dispersion of Nanoparticles for Strengthening Cast Aluminum Alloy A 356, *Metall. Sci. Technol.*, 2008, **26**, p 2
17. Yong Yang and Xiaochun Li, Ultrasonic Cavitation Based Nanomanufacturing of Bulk Aluminum Matrix Nanocomposites, *Trans. ASME Ser. B*, 2007, **129**, p 497–501
18. G. Cao, H. Konishi, and X. Li, Recent Developments on Ultrasonic Cavitation Based Solidification Processing of Bulk Magnesium Nanocomposites, *Int. J. Metalcast.*, 2008, **8**, p 58–65
19. A. Erman, J. Groza, X. Li, H. Choi, and G. Cao, Nanoparticle Effects in Cast Mg-1wt% SiCNano-Composites, *Mater. Sci. Eng. A*, 2012, **558**, p 39–43
20. G. Cao, J. Kobliska, H. Konishi, and X. Li, Tensile Properties and Microstructure of SiC Nanoparticle-Reinforced Mg-4Zn Alloy Fabricated by Ultrasonic Cavitation-Based Solidification Processing, *Metall. Mater. Trans. A*, 2008, **39**, p 880–886
21. G. Cao, H. Choi, H. Konishi, S. Kou, R. Lakes, and X. Li, Mg–6Zn/1.5% SiC Nanocomposites Fabricated by Ultrasonic Cavitation-Based Solidification Processing, *J. Mater. Sci.*, 2008, **43**, p 5521–5526
22. G. Cao, H. Konishi, and X. Li, Mechanical Properties and Microstructure of SiC-Reinforced Mg-(2,4)Al-1Si Nanocomposites Fabricated by Ultrasonic Cavitation Based Solidification Processing, *Mater. Sci. Eng. A*, 2008, **486**, p 357–362
23. S. Mula, P. Padhi, S.C. Panigrahi, S.K. Pabi, and S. Ghosh, On Structure and Mechanical Properties of Ultrasonically Cast Al–2% Al_2O_3 Nanocomposite, *Mater. Res. Bull.*, 2009, **44**, p 1154–1160
24. C. Dengbin, Z. Yutao, L. Guirong, Z. Meng, and C. Gang, Mechanism and Kinetic Model of In-Situ TiB2 7055Al Nanocomposites Synthe-

sized Under High Intensity Ultrasonic Field, *J. Wuhan Univ. Technol., Mater. Sci. Ed.*, 2011, **26**, p 920–925
25. M.C. Arenas, L.F. Rodriguez-Nunez, D. Rangel, O. Martinez-Alvarez, C. Martinez-Alonso, and V.M. Castano, Simple One-Step Ultrasonic Synthesis of AnataseTitania/Polypyrrole Nanocomposites, *Ultrason. Sonochem.*, 2013, **20**, p 777–784
26. K. Ullah, S. Ye, S.-B. Jo, L. Zhu, K.-Y. Cho, and W.-C. Oh, Optical and Photocatalytic Properties of Novel Heterogeneous $PtSe_2$-Graphene/TiO_2 Nanocomposites Synthesized via Ultrasonic Assisted Techniques, *Ultrason. Sonochem.*, 2014, doi:10.1016/j.ultsonch.2014.04.016
27. G. Chen, W. Weng, D. Wu, C. Wu, J. Lu, P. Wang, and X. Chen, Preparation and Characterization of Graphite Nanosheets, *Carbon*, 2004, **42**, p 753–759
28. M. Lotya, Y. Hernandez, P.J. King, R.J. Smith, V. Nicolosi, L.S. Karlsson, F.M. Blighe, S. De, Z. Wang, I.T. McGovern, G.S. Duesberg, and J.N. Coleman, Liquid Phase Production of Graphene by Exfoliation of Graphite in Surfactant/Water Solutions, *J. Am. Chem. Soc.*, 2009, **131**, p 3611–3620
29. J.H. Warner, Chemical Exfoliation, Methods for Obtaining Graphene, *Graphene*, 2013, doi:10.1016/B978-0-12-394593-8.00004-7
30. Y. Geng, S.J. Wang, and J.-K. Kim, Preparation of Graphite Nanoplatelets and Graphene Sheets, *J. Colloid Interface Sci.*, 2009, **336**, p 592–598
31. S. Castarlenas, C. Rubio, A. Mayoral, C. Tellez, and J. Coronas, Few-layer Graphene by Assisted-Exfoliation of Grapite with Layered Silicate, *Carbon*, 2014, doi:10.1016/j.carbon.2014.02.044
32. G. Ramani, R.M. Pillai, B.C. Pai, and T.R. Ramamohan, Factors Affecting the Stability of Non-wetting Dispersoid Suspensions in Metallic Melts, *Composites*, 1991, **22**(2), p 143–150
33. J. Banhart, Manufacture, Characterisation and Application of Cellular Metals and Metal Foams, *Prog. Mater. Sci.*, 2001, **46**, p 559–632
34. K.S. Suslick, Y. Didenko, M.M. Fang, T. Hyeon, K.J. Kolbeck, W.B. McNamara, M.M. Mdleleni, and M. Wong, Acoustic Cavitation and Its Chemical Consequences, *Phil. Trans. R. Soc. Lond. A*, 1999, **357**, p 335–353
35. G.I. Eskin, Cavitation Mechanism of Ultrasonic Melt Degassing, *Ultrason. Sonochem.*, 1995, **2**(2), p 137–141
36. N. Alba-Baena, D. Eskin, Kinetics of Ultrasonic Degassing of Aluminium Alloys, TMS, 2013, p 957–962
37. H. Puga, J. Barbosa, J.C. Teixeira, and M. Prokic, A New Approach to Ultrasonic Degassing to Improve the Mechanical Properties of Aluminum Alloys, *J. Mater. Eng. Perform.*, 2014, **23**, p 3736–3744
38. H. Xu, X. Jian, T.T. Meek, and Q. Han, Degassing of Molten Aluminum A356 Alloy Using Ultrasonic Vibration, *Mater. Lett.*, 2004, **58**, p 3669–3673
39. H. Xu and K.S. Suslick, Sonochemical Preparation of Functionalized Graphenes, *J. Am. Chem. Soc.*, 2011, **133**, p 9148–9151
40. V. Stengl, Preparation of Graphene by Using an Intense Cavitation Field in Pressurized Ultrasonic Reactor, *Chem. Eur. J.*, 2012, doi: 10.1002/chem.201201411
41. T.D. Burchell, Graphite: Properties and Characteristics. *Compr. Nucl. Matr.*, 2012, **2**, p 285–305